Differentiation of Isomers by Wavelength-Tunable Infrared Multiple-Photon Dissociation-Mass Spectrometry: Application to Glucose-Containing Disaccharides

ARTICLE *in* ANALYTICAL CHEMISTRY · MARCH 2006

Impact Factor: 5.64 · DOI: 10.1021/ac0519458 · Source: PubMed

6 AUTHORS, INCLUDING:

Nicolas Polfer
University of Florida
81 PUBLICATIONS **2,961** CITATIONS
SEE PROFILE

David T Moore
Lehigh University
53 PUBLICATIONS **1,624** CITATIONS
SEE PROFILE

John R Eyler
University of Florida
178 PUBLICATIONS **4,184** CITATIONS
SEE PROFILE

Anal. Chem. **2006,** *78,* 670−679

Differentiation of Isomers by Wavelength-Tunable Infrared Multiple-Photon Dissociation-Mass Spectrometry: Application to Glucose-Containing Disaccharides

Nick C. Polfer,*,† Jose J. Valle,‡ David T. Moore,† Jos Oomens,† John R. Eyler,‡ and Brad Bendiak§

FOM Institute for Plasma Physics, 'Rijnhuizen', Molecular Dynamics Group, Edisonbaan 14, 3439 MN Nieuwegein, The Netherlands, Department of Chemistry, University of Florida, Gainesville, Florida 32611-7200, and Department of Cellular and Developmental Biology and Biomolecular Structure Program, University of Colorado Health Sciences Center, Aurora, Colorado 80010-7163

Variation in the wavelength of irradiation in infrared multiple-photon dissociation (IR-MPD) of lithium-tagged glucose-containing disaccharide ions (1−2-, 1−3-, 1−4-, and 1−6-linked isomers of both anomeric configurations) resulted in marked differences in their mass spectral fragmentation patterns. Two-dimensional plots of the fragment yield versus infrared wavelength for each mass spectral product ion were unique for each isomer and can be considered a spectral fingerprint. Individual product ions or diagnostic ratios of key product ions can be optimized at specific IR wavelengths. The technique permits both linkage position and anomeric configuration to be assigned. The ratio of the fragments derived by cleavage at the glycosidic bond (*m/z* 169/187) is much enhanced for *β*-anomers compared to α-anomers. Differences in the diagnostic product ions 169 and 187 were largest in the range of 9.0−9.4 *μ*m, where the maximum dissociation yield was observed. Conversely, at 10.6 *μ*m, the wavelength of nontunable CO_2 lasers that accompany commercial Fourier transform ion cyclotron resonance mass spectrometers, the dissociation yield was poor and anomeric differentiation was not possible. In contrast to previous studies by collision-induced dissociation, the trends in dissociation behavior between anomers using IR-MPD are significant and allow simple diagnostic rules to be established. By depositing energy into these isobaric ions via narrow-band IR excitation, the resulting internal energy can be finely controlled, thereby obtaining high reproducibility in dissociation patterns. Given the multidimensionality of variable-wavelength IR-MPD of lithiated disaccharides, it is expected that this approach can overcome some of the current limitations in isomer differentiation.

The isomeric differentiation of oligosaccharides remains an ongoing challenge for mass spectrometry, yet a vital one, as they play crucial roles in ligand−receptor interactions during development and in various cell recognition, adherence, motility, and signaling processes.[1−4] Since oligosaccharides represent an extreme case of isomeric heterogeneity among molecules, with 80−90% of carbons being chiral in addition to having positional (linkage) isomers, their isomeric differentiation is a particularly useful test case for application of advanced mass spectrometric techniques. When ions are not exact compositional isomers, Fourier transform ion cyclotron resonance (FTICR) instruments[5] can often resolve them based on minute differences in *m/z*. However, when ions have identical elemental compositions, some other physical property must be exploited to differentiate between them. Such properties include changes in their fragmentation patterns,[6−8] differences in their rates of migration through a gas (ion mobility spectrometry[9−12] or field asymmetric waveform ion mobility spectrometry[13]), differences in reactivity,[14−17] differences

* To whom correspondence should be addressed. E-mail: polfer@rijnh.nl.
† FOM Institute for Plasma Physics.
‡ University of Florida.
§ University of Colorado Health Sciences Center.

(1) Hennet, T.; Ellies, L. G. *Biochim. Biophys. Acta* **1999**, *1473*, 123−136.
(2) Gabius, H. J.; Andre, S.; Kaltner, H.; Siebert, H.-C. *Biochim. Biophys. Acta* **2002**, *1572*, 165−177.
(3) Hakomori, S.-I. In *The molecular immunology of complex carbohydrates*, 2 ed.; Wu, A. M., Ed.; Plenum Press: New York, 2001; pp 369−402.
(4) Taylor, M. E.; Drickamer, K. *Introduction to glycobiology*; Oxford University Press: Oxford, U.K., 2003.
(5) Marshall, A. G. *Int. J. Mass Spectrom.* **2000**, *200*, 331−356.
(6) Zhou, Z.; Ogden, S.; Leary, J. A. *J. Org. Chem.* **1990**, *55*, 5444−5446.
(7) Hofmeister, G. E.; Zhou, Z.; Leary, J. A. *J. Am. Chem. Soc.* **1991**, *113*, 5964−5970.
(8) Asam, M. R.; Glish, G. L. *J. Am. Soc. Mass Spectrom.* **1997**, *8*, 987−995.
(9) Liu, Y.; Clemmer, D. E. *Anal. Chem.* **1997**, *69*, 2504−2509.
(10) Wu, C.; Siems, W. F.; Asbury, G. R.; Hill, H. H. J. *Anal. Chem.* **1998**, *70*, 4929−4938.
(11) Hoaglund-Hyzer, C. S.; Clemmer, D. E. *Anal. Chem.* **2001**, *73*, 177−184.
(12) Clowers, B. H.; Dwivedi, P.; Steiner, W. E.; Hill, H. H. J.; Bendiak, B. *J. Am. Soc. Mass Spectrom.* **2005**, *16*, 660−669.
(13) Barrett, D. A.; Ells, B.; Guevremont, R.; Purves, R. W. *J. Am. Soc. Mass Spectrom.* **1999**, *10*, 1279−1284.
(14) Nourse, B. D.; Hettich, R. L.; Buchanan, M. V. *J. Am. Soc. Mass Spectrom.* **1993**, *4*, 296−305.
(15) Sharifi, M.; Einhorn, J. *Int. J. Mass Spectrom.* **1999**, *191*, 253−264.
(16) Petucci, C.; Guler, L.; Kenttamaa, H. I. *J. Am. Soc. Mass Spectrom.* **2002**, *13*, 362−370.
(17) Gao, H.; Petzold, C. J.; Leavall, M. D.; Leary, J. A. *J. Am. Soc. Mass Spectrom.* **2003**, *14*, 916−924.

10.1021/ac0519458 CCC: $33.50
Published on Web 12/24/2005

in mass analyzed ion kinetic energy (MIKE) spectra of metastable ions[18,19] or any other spectroscopic difference observable between them, which could include direct photon absorption[20,21] or emission[22] spectra of trapped gas-phase ions. The fragmentation of isomers represents the most thoroughly studied approach; however, often the differences in fragmentation patterns between the isomers are too small to distinguish between a large number of variants.

Control of dissociation of selected ions in mass spectrometry is a topic of fundamental theoretical concern and of great practical importance. In collisions of ions with particles at moderate kinetic energies, including electrons, neutral gas atoms, or molecules, the energy deposition usually shows a fairly broad distribution, depending on factors such as relative velocities, angle, impact parameter (a "glancing blow" as compared to a "head-on collision"), and the mass and nature of the collision partner. Kim and McLafferty have used statistical methods to calculate the collisional energy probability functions for energy transfer to ions using collision-induced dissociation (CID),[23] which can cover energies comparable to rotational/vibrational energies up to UV (ultraviolet) energies using a single relative velocity. Consequently, for most collision processes, precise control of energy transfer to an ion is inherently difficult to achieve. Note that for single-collision processes, such as employed in threshold collision-induced dissociation (TCID),[24] very accurate selection of energy-transfer processes is possible, even allowing binding energies of noncovalently bound systems to be determined.

An alternative means to excite an ion is through absorption of photons; in fact, photodissociation of trapped ions using UV, visible, or IR (infrared) light is a well-established technique.[20,25−29] As compared to CID, the absorption of photons has one crucial advantage in selective control of fragmentation, in that the fragmentation is wavelength-dependent, thus adding another dimension to the experimental data. Infrared multiple-photon dissociation (IR-MPD)[30] has advantages over the use of UV or visible light irradiation and over CID dissociation methods (other than in the special case of TCID) in that the *energy distribution* of the excited ions is much narrower.[31] In IR-MPD, typically the absorption of tens to hundreds of photons is necessary to reach the fragmentation thresholds of molecular ions and induce dissociation, which requires the use of high fluence lasers. This process is mediated by intramolecular vibrational redistribution[32] with a net buildup in internal energy. When an ensemble of identical selected ions moves through a collimated IR beam of narrow bandwidth, obviously not all ions absorb the same number of photons and thus there is a distribution in internal energies, which follows Poisson statistics and depends on the mean number of photons absorbed and the energy per photon. At mid-infrared wavelengths, the distribution in internal energy is considerably narrower than the corresponding thermal distribution that would be expected for collisional activation of an ensemble of ions using multiple collision events,[32] and compared to UV or visible wavelengths, the energy distribution in IR-MPD is narrower, because the energy per photon is much lower.[31] Currently, free electron lasers (FELs)[33] are among the only stable high-power IR sources tunable over broad frequency ranges that allow dissociation of ions in a wavelength-specific manner.[34−38] The laser fluence for FELs can be accurately controlled, which is crucial, given the IR-MPD yield dependence on fluence.

A plethora of competing MS approaches have been investigated for oligosaccharides, in both the positive and negative ion modes.[39,40] At this time, alternate methods, including fragmentation after derivatization,[41] are all valuable because they can provide overlaps in coverage for structural determination. In the positive ion mode, protonated oligosaccharides tend to provide the least information as cleavage occurs almost exclusively at glycosidic linkage sites.[42] For alkali metal adducts, whereas Li^+-bound oligosaccharides give cross-ring cleavage fragments, Cs^+-bound structures, for example, exclusively give rise to loss of the cesium cation.[42,43] This is due to the decreased binding strength of alkali-metal complexes from Li^+ to Cs^+ [42,44] and the inability of larger ions to effect charge-induced dissociation.[42,43] Lithiated oligosaccharides also give the highest ionization yield,[45] thus making Li^+ one of the more useful metal cations in carbohydrate MS analysis. Disaccharides represent the smallest isolable substructures of larger oligosaccharides that still contain a glycosidic linkage between monosaccharides. Important information about the fragmentation of lithiated disaccharides has been provided through

(18) Kralj, B.; Kramer, V.; Zigon, D.; Kobe, J.; Stimac, A. *Rapid Commun. Mass Spectrom.* **1993**, *7*, 147−151.
(19) Smith, G.; Leary, J. A. *J. Am. Soc. Mass Spectrom.* **1996**, *7*, 953−957.
(20) Dunbar, R. C. *Int. J. Mass Spectrom.* **2000**, *200*, 571−589.
(21) Duncan, M. A. *Int. J. Mass Spectrom.* **2000**, *200*, 545−569.
(22) Wang, Y.; Hendrickson, C. L.; Marshall, A. G. *Chem. Phys. Lett.* **2001**, *334*, 69−75.
(23) Kim, M. S.; McLafferty, F. W. *J. Am. Chem. Soc.* **1978**, *100*, 3279−3282.
(24) Rodgers, M. T.; Armentrout, P. B. *Mass Spectrom. Rev.* **2000**, *19*, 215−247.
(25) Dunbar, R. C. In *Gas-Phase Ion Chemistry*; Bowers, M. T., Ed.; Academic Press: New York, 1979; Vol. 2, pp 180−220.
(26) Thorne, L. R.; Beauchamp, J. L. In *Gas-Phase Ion Chemistry*; Bowers, M. T., Ed.; Academic Press: New York, 1984; Vol. 3, p 41.
(27) Baykut, G.; Watson, C. H.; Weller, R. R.; Eyler, J. R. *J. Am. Chem. Soc.* **1985**, *107*, 8036−8042.
(28) Peiris, D. M.; Cheeseman, M. A.; Ramanathan, R.; Eyler, J. R. *J. Phys. Chem.* **1993**, *97*, 7839−7843.
(29) Dibben, M. J.; Kage, D.; Szczepanski, J.; Eyler, J. R.; Vala, M. *J. Phys. Chem.* **2001**, *105*, 6024−6029.
(30) Bagratashvili, V. N.; Letokov, V. S.; Makarov, A. A.; Ryabov, E. A. *Multiple Photon Infrared Laser Photophysics and Photochemistry* Harwood: Churchester, 1985.
(31) von Helden, G.; van Heijnsbergen, D.; Meijer, G. *J. Phys. Chem. A* **2003**, *107*, 1671−1688.
(32) Grant, E. R.; Schulz, P. A.; Sudbo, A. S.; Shen, Y. R.; Lee, Y. T. *Phys. Rev. Lett.* **1978**, *40*, 115−118.
(33) Colson, W. B.; Johnson, E. D.; Kelley, M. J.; Schwettmann, H. A. *Phys. Today* **2002**, *55*, 35−41.
(34) Oomens, J.; Moore, D. T.; von Helden, G.; Meijer, G.; Dunbar, R. C. *J. Am. Chem. Soc.* **2004**, *26*, 724−725.
(35) Kapota, C.; Lemaire, J.; Maitre, P.; Ohanessian, G. *J. Am. Chem. Soc.* **2004**, *126*, 1836−1842.
(36) Valle, J. J.; Eyler, J. R.; Oomens, J.; Moore, D. T.; van der Meer, A. F. G.; von Helden, G.; Meijer, G.; Hendrickson, C. L.; Marshall, A. G.; Blakney, G. T. *Rev. Sci. Instrum.* **2005**, *76*, 23103.
(37) Moore, D. T.; Oomens, J.; Eyler, J. R.; von Helden, G.; Meijer, G.; Dunbar, R. C. *J. Am. Chem. Soc.* **2005**, *127*, 7243−7254.
(38) Polfer, N.; Paizs, B.; Snoek, L. C.; Compagnon, I.; Suhai, S.; Meijer, G.; von Helden, G.; Oomens, J. *J. Am. Chem. Soc.* **2005**, *127*, 8571−8579.
(39) Zaia, J. *Mass Spectrom. Rev.* **2004**, *23*, 161−227.
(40) Park, Y. M.; Lebrilla, C. B. *Mass Spectrom. Rev.* **2005**, *24*, 232−264.
(41) Sheeley, D. M.; Reinhold, V. *Anal. Chem.* **1998**, *70*, 3053−3059.
(42) Ngoka, L. C.; Gal, J.-F.; Lebrilla, C. B. *Anal. Chem.* **1994**, *66*, 692−698.
(43) Cancilla, M. T.; Penn, S. G.; Carroll, J. A.; Lebrilla, C. B. *J. Am. Chem. Soc.* **1996**, *118*, 6736−6745.
(44) Bothner, B.; Carmichael, L.; Staniszewski, K.; Sonderegger, M.; Siuzdak, G. *Spectroscopy* **2002**, *16*, 71−79.
(45) Harvey, D. J. *J. Mass Spectrom.* **2000**, *35*, 1178−1190.

earlier CID studies, some of which employed ^{18}O labeling of the carbonyl oxygen of the reducing sugar so that the source of each ion could be readily identified.[6−8] Conclusions from these studies were that diagnostic cross-ring cleavages occur that characterize the linkage position between two sugars. This has also been observed for deprotonated disaccharides in the negative ion mode.[46,47] IR-MPD has been previously utilized at a single wavelength, the major emission line of a CO_2 laser, 10.6 μm, to fragment saccharomicins,[48] glycopeptide oligosaccharides,[49] and alkali metal-coordinated oligosaccharides and oligosaccharide alditols.[50,51] These studies demonstrated that IR absorption at this wavelength will fragment carbohydrates and that Li^+ and Na^+ remain attached to product ions.

Less work, however, has been carried out on differentiation of anomeric configuration by MS. It has been shown that carbohydrate anomers can be identified by MIKE MS;[18,19] the intensity ratios of diagnostic peaks during in-source decay in negative ion ESI has permitted anomeric differentiation;[52,53] CID studies of chloride-tagged disaccharides have shown that there are differences in fragmentation between anomers;[54] derivatization with ethers of increasing bulkiness has enabled some anomers to be discriminated.[55] As yet, however, no routine MS technique exists to establish anomeric configuration in oligosaccharides, which is due either to the absence of consistent trends in fragmentation between anomers of different stereoisomers or simply to the fact that many stereochemical variants have not been examined (for example, more rare aldohexoses such as altrose, allose, gulose, or talose would certainly be possible candidates in natural oligosaccharides). With such a large number of possible isomeric variants, even elucidation of an unknown disaccharide can be a significant challenge for MS alone (without hydrolysis to monomers and some form of chromatography such as GC). Here we demonstrate that IR-MPD[30] furnishes marked differences in fragmentation of disaccharides at different wavelengths. Two-dimensional IR irradiation-mass spectra (IRI-MS) are unique for each disaccharide and enable both linkage position and anomeric configuration to be assigned.

EXPERIMENTAL SECTION

Disaccharides ($C_{12}H_{22}O_{11}$) were composed solely of D-glucose (Glc), and the nonreducing monosaccharide was in pyranoside ring form. Sophorose (Glcβ1−2Glc) was from Serva Chemicals. Kojibiose (Glcα1−2Glc) was purchased from Koch-Light Ltd. Other disaccharides having trivial names laminaribiose (Glcβ1−3Glc), nigerose (Glcα1−3Glc), cellobiose (Glcβ1−4Glc), maltose (Glcα1−4Glc), gentiobiose (Glcβ1−6Glc), and isomaltose (Glcα1−6Glc) were from Sigma-Aldrich. Samples were made up at a concentration of 1 mM mixed with 1 mM LiCl in MeOH/H_2O (80:20) solutions. The lithiated disaccharides were generated using electrospray ionization (ESI) using a commercial ESI source (Micromass, Manchester, U.K.), which was fitted to a laboratory-built FTICR mass spectrometer described in detail elsewhere.[36] Ions were accumulated in a storage hexapole (200−300 ms) and then pulse-extracted, moving through a quadrupole deflector (ABB Extrel) and an octopole ion guide, into the ICR cell where they were trapped.

Here, the lithiated precursor ion (m/z 349) was mass isolated and then irradiated with macropulses from the *f*ree *e*lectron *l*aser for *i*nfrared e*x*periments (FELIX).[56] Typically 20 macropulses at 10-Hz repetition rate were used, equaling a storage time for irradiation of 2 s. FELIX is capable of delivering high-energy macropulses (60 mJ) of infrared light over a very wide wavelength region (5−250 μm) and a full width at half-maximum (fwhm) bandwidth of typically 0.5% of the central wavelength (e.g., 5 cm^{-1} at 1000 cm^{-1}). In these experiments, the wavelength of FELIX was scanned between 7 and 11 μm (~1400−900 cm^{-1}) and the IR-MPD yield was monitored as a function of wavelength. The IR-MPD yield was normalized to the total number of ions in the ICR trap and the laser fluence at a particular wavelength. The pulse structure of a free electron laser reflects the timing of electron bunches employed in the generation of light. In these experiments, FELIX was operated at 1 GHz, which means that picosecond-long micropulses of IR light were generated that are spaced by 1 ns; a whole pulse-"train" of these micropulses makes up a macropulse, which is 4−5 μs in length. Note that this pulse structure particularly suits the application of IR-MPD: within the time scale of a macropulse (i.e., a few microseconds), a particular ion hardly moves relative to the laser focus in an ion trapping MS and is therefore available to absorb light from multiple micropulses. Furthermore, given the very high density of states of polyatomic biomolecules, when a photon is absorbed in one micropulse, this energy is quickly transferred to other vibrational states (picosecond time scale) during the 1-ns period to the following micropulse and hence the molecule is capable of absorbing another photon at the fundamental frequency.

RESULTS AND DISCUSSION

Variation in Fragmentation of Disaccharides with the Wavelength of Infrared Irradiation. Product ions were monitored as a set of m/z channels derived from precursor ions of m/z 349 for isomeric lithium-cationized disaccharides. Data sets were accumulated using IR-MPD at different IR wavelengths over the range from 7 to 11 μm. The data for each dissociation channel can be represented in two dimensions (Figure 1). Results are shown from two 3-linked isomers of glucose-containing disaccharides having different anomeric configurations, and proposed cleavages are illustrated in Figure 2b. Immediately apparent in these 2D IRI-MS two-dimensional infrared irradiation mass spectra (Figure 1) are the differences in fragmentation at different IR wavelengths, where the ratios ofproduct ions at each wavelength

(46) Garozzo, D.; Giuffrida, M.; Impallomeni, G.; Ballistreri, A.; Montaudo, G. *Anal. Chem.* **1990**, *62*, 279−286.
(47) Dallinga, J. W.; Heerma, W. *Biol. Mass Spectrom.* **1991**, *20*, 215−231.
(48) Shi, S. D. H.; Hendrickson, C. L.; Marshall, A. G.; Siegel, M. M.; Kong, F.; Carter, G. T. *J. Am. Soc. Mass Spectrom.* **1999**, *10*, 1285−1290.
(49) Hakansson, K.; Cooper, H. J.; Emmett, M. R.; Costello, C. E.; Marshall, A. G.; Nilsson, C. L. *Anal. Chem.* **2001**, *73*, 4530−4536.
(50) Xie, Y.; Lebrilla, C. B. *Anal. Chem.* **2003**, *75*, 1590−1598.
(51) Zhang, J.; Schubothe, K.; Li, B.; Russel, S.; Lebrilla, C. B. *Anal. Chem.* **2005**, *77*, 208−214.
(52) Mulroney, B.; Traeger, J. C.; Stone, B. A. *J. Mass Spectrom.* **1995**, *30*, 1277−1283.
(53) Mulroney, B.; Peel, J. B.; Traeger, J. C. *J. Mass Spectrom.* **1999**, *34*, 856−871.
(54) Jiang, Y.; Cole, R. B. *J. Am. Soc. Mass Spectrom.* **2005**, *16*, 60−70.
(55) Mendonca, S.; Cole, R. B.; Zhu, J.; Cai, Y.; French, A. D.; Johnson, G. P.; Laine, R. A. *J. Am. Soc. Mass Spectrom.* **2005**, *14*, 63−78.
(56) Oepts, D.; van der Meer, A. F. G.; van Amersfoort, P. W. *Infrared phys. technol.* **1995**, *36*, 297−308.

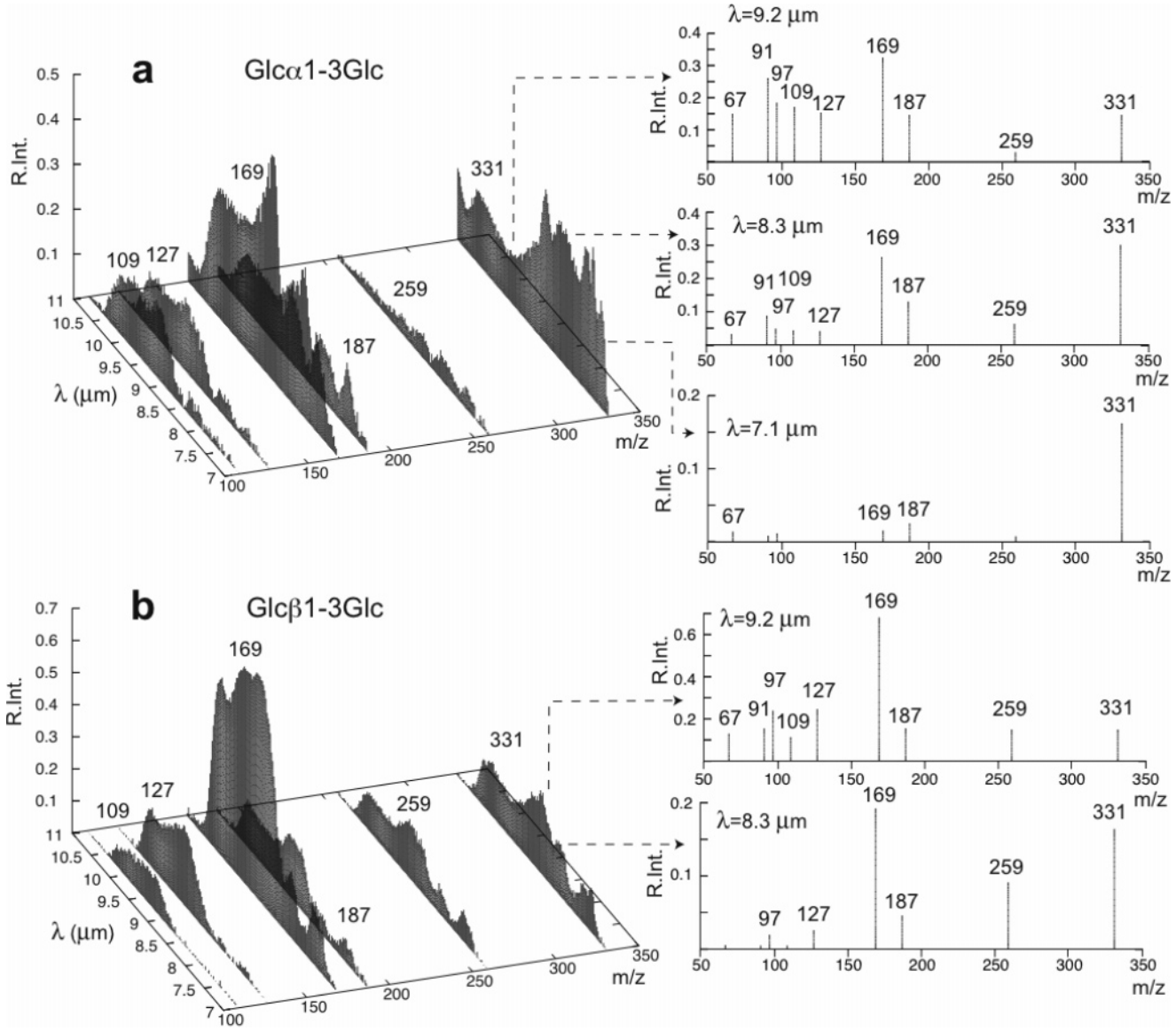

Figure 1. Two-dimensional IRI-MS infrared irradiation mass spectra of two lithium-tagged glucose-containing disaccharides (left) and mass spectra extracted from the 2D data set at selected IR wavelengths (right). Relative intensities of ions are indicated along the vertical axis (R. Int.). Spectra were obtained from the precursor ions of anomeric isomers of *m*/*z* 349, the Li^+ adducts of (a) nigerose, Glcα1−3Glc, and (b) laminaribiose, Glcβ1−3Glc. The IR irradiation wavelength of each selected mass spectrum is shown above for each 1D plot. At 7.1 μm, product ion abundance was negligible for laminaribiose, so this plot was not shown for (b). For clarity of presentation, low *m*/*z* product ions (*m*/*z* <100) are not shown for the 2D spectra, but their abundance was observed to be wavelength-dependent.

were highly reproducible. These 2D spectra are unique fingerprints for the disaccharides studied. As shown in 1D mass spectra extracted from these 2D plots, differences in fragmentation often represent more than simply differences in product ion ratios; at some IR wavelengths, certain product ions were not observed at all. For example, upon irradiation of the lithium−nigerose adduct (Glcα1−3Glc) at 7.1 μm (Figure 1a), by far the most abundant product ion was found at *m*/*z* 331, due to a single water loss. Low quantities of product ions were observed that were derived by cleavages on either side of the glycosidic oxygen (*m*/*z* 169 or 187), and low quantities of product ions were observed having *m*/*z* less than 150, with two of these (*m*/*z* 109 and 127) not being observed at all, although they were observed at other IR wavelengths. In contrast, at 8.3 μm, maximal abundance of the diagnostic cross-ring ion *m*/*z* 259 was observed, along with a series of other ions including the *m*/*z* 331 ion and higher quantities of ions derived by breakage on either side of the glycosidic oxygen as well as other lower *m*/*z* ions. At 9.2 μm, far more of the fragments of low *m*/*z* were observed. The profile with laminaribiose (Glcβ1−3Glc, Figure 1b) was quite different: at 8.3 μm, higher amounts of ions due to cross-ring (*m*/*z* 259) and glycosidic bond cleavage (*m*/*z* 169) were seen as compared to nigerose. At 9.2 μm, these same ions were also more abundant than for nigerose, and the lower *m*/*z* product ions (*m*/*z* <150) differed in their relative abundances. At 7.1 μm, essentially no dissociation occurred with laminaribiose. These data clearly indicate that variation in fragmentation occurs that is dependent on the wavelength of IR irradiation. Fragmentation patterns were characteristic of isomers under investigation and demonstrate that the abundance of the most structurally informative product ions can be optimized at specific wavelengths.

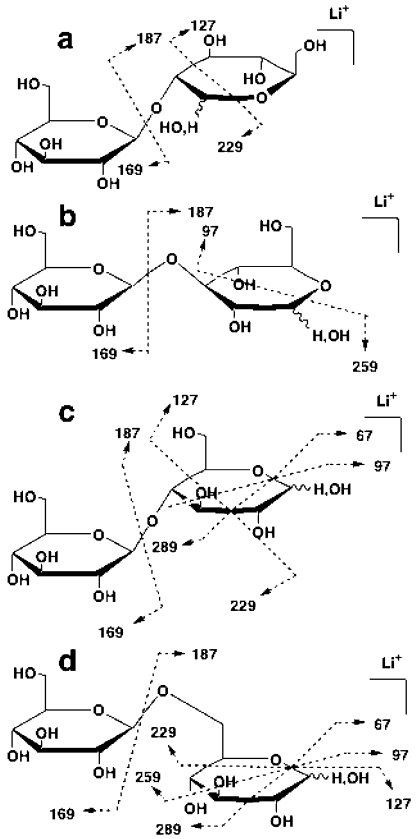

Figure 2. Proposed cleavages for lithium-cationized disaccharides having different linkages. (a) Glcβ1−2Glc, (b) Glcβ1−3Glc, (c) Glcβ1−4Glc, and (d) Glcβ1−6Glc. Proposed fragmentation of the reducing sugar is based on previous studies of lithiated disaccharides using ^{18}O labeling of the reducing sugar carbonyl group.[7,8]

Differentiation of Disaccharide Linkage Isomers. Two-dimensional IRI-MS are shown for the other isomers of glucose-containing disaccharides having 1−2, 1−4, and 1−6 linkages (Figure 3). Linkage isomers can be distinguished because the sets of cross-ring cleavages that generate ions with larger m/z than monosaccharides (m/z 229, 259, 289 and 331) are characteristic of the linkages (Tables 1 and 2). Previous studies using CID also showed these diagnostic fragments, and with ^{18}O-labeled disaccharides having either 1−4 or 1−6 linkages, it was established that water loss and cross-ring cleavages occurred on the reducing sugar.[7,8] The m/z 187 ion (189 with carbonyl ^{18}O labeling) was derived from the reducing monosaccharide whereas the m/z 169 ion was derived from the nonreducing sugar.[57] As other ions (m/z 127, 109, 97, 91 and 67) were not previously reported, verifications of their origin(s) await isotopic labeling studies. The cleavages shown to generate these latter ions in Figure 2 are tentative as it is possible that they originate from cleavage of the nonreducing sugar. Also, these fragmentation schemes are incomplete; they do not account for some of the observed fragments (e.g., m/z 127 in the case of a 3-linked disaccharide, m/z 109 and 91 for all structures).

Optimization of Spectral Differences. Examination of the 2D IRI-MS in more detail reveals that the optimal ratios of the diagnostic cross-ring ions occur at specific wavelengths so their abundance can be favored relative to that of less structurally informative ions. For the 2-linked disaccharides, the single cross-ring ion of m/z 229 was found in highest abundance relative to other ions at an irradiation wavelength near 7.6 μm. For 4-linked structures, optimal cross-ring product ions (m/z 289 and 229) relative to other product ions were found near 8.7 μm, whereas for 6-linked fragments this value (for m/z 289, 259 and 229) was near 8.3 μm. Although overall higher cross-ring cleavage ion yields were observed between 9.1 and 9.4 μm for the 6-linked structures, higher *relative* amounts of ions were also observed resulting from glycosidic bond cleavage and fragmentation into smaller m/z ions. The practical utility of selecting specific wavelengths over others depends in part on the optimal ratio of selected product ion channels to the additive amounts in all other channels. For some purposes, absolute quantities of key product ions may be desired, which may be at a different wavelength than that giving the highest relative product ion ratio.

Discrimination between Anomeric Configuration of Isomers. For the glucose-containing disaccharides examined, each 2D IRI-MS differs between anomers, so that the anomeric configuration can be readily identified by matching the 2D spectra. A trend was observed in the ratios of the m/z 169/187 ions when comparing the α/β anomers for all disaccharides tested. Disaccharides with a β-linkage between monosaccharide units had a significantly higher ratio of m/z 169/187 product ions than their α-linked counterparts with the same linkage position. This was observed over most wavelengths that led to dissociation although the maximum difference was observed between about 8.8 and 9.6 μm, depending on the specific disaccharide (Figure 4). The differences in m/z 169/187 ratios decreased on either side of the maximum and were minimal at the edges of the main absorption band. Quantitative values for the m/z 169 and 187 product ions at fixed wavelengths of 9.2 and 9.6 μm are presented (Tables 1 and 2). These wavelengths were chosen since the fragment ion abundances in experiments were reasonably high in this range and efficient laser lines are available at 9.2 and 9.6 μm for CO_2 lasers using a moveable diffraction grating. With anomers having the same linkage position compared as pairs, the m/z 169/187 fragment intensity ratios ranged from a 2- to 9-fold increase for the β-anomers as compared to the α-anomers. Given the high abundance of these fragment channels in the range of 8.8−9.6 μm, their relative ratios can be accurately determined and hence the disaccharide anomeric configuration can be assigned. It is premature to generalize a correlation of the m/z 169/187 ion pairs to any other monosaccharide anomeric configurations in disaccharides although unique 2D IRI-MS spectra for each anomeric pair would be expected.

Reproducibility and Other Experimental Concerns. These results prompted five questions. (1) How reproducible are the IR-MPD spectra? (2) Which experimental parameters affect the reproducibility? (3) Do some of the ions result from secondary fragmentation of product ions and how does that affect

(57) The ^{18}O labeling study (ref 7) clearly demonstrated that the glycosidic bond cleavage predominantly takes place with the glycosidic oxygen retained on the reducing sugar thereby explaining the high-abundance 189 peak in the CID mass spectrum of lithiated gentiobiose. A smaller peak on the left-hand side of the 189 peak (187?) could be rationalized by glycosidic bond cleavage with retention of the oxygen with the nonreducing sugar. While both cleavages can occur, the former mechanism is much more prevalent in the case of lithiated gentiobiose.

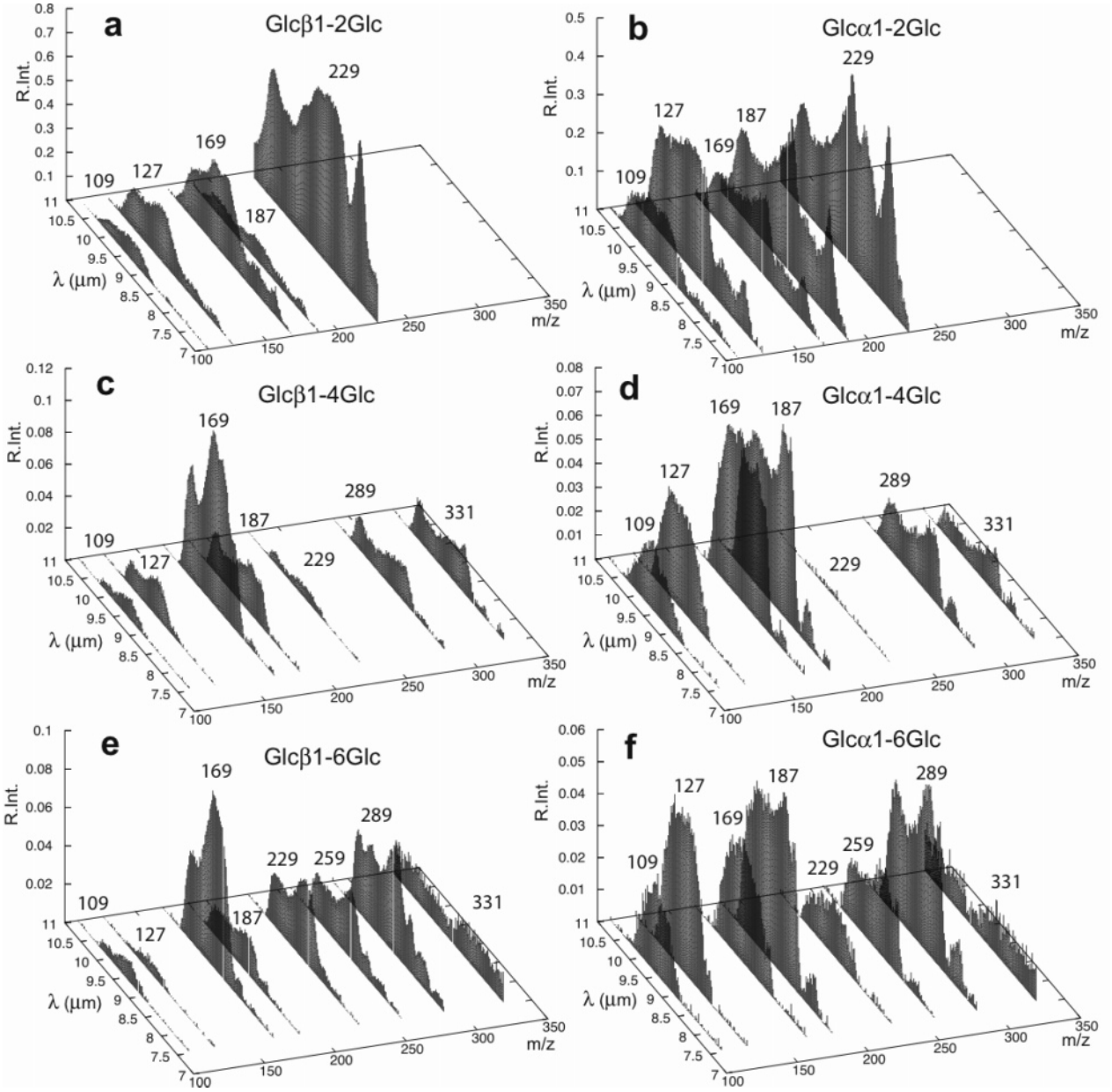

Figure 3. Two-dimensional IRI-MS of lithium-tagged glucose-containing disaccharides. Spectra are obtained from the precursor ions of anomeric isomers having *m*/*z* 349. Anomeric pairs are shown alongside each other. Panels: (a), sophorose, (b) kojibiose, (c) cellobiose, (d) maltose, (e) gentiobiose, and (f) isomaltose. Other low *m*/*z* ions (*m*/*z* 97, 91, 67) were not shown for clarity of presentation, but their abundance was also wavelength-dependent.

reproducibility and interpretation of data? (4). Are the parent ions a mixture with lithium complexation occurring at more than one site? (5) What are the overall dissociation yields at different IR frequencies (additive amounts of all product ions) and how effective is the standard 10.6-μm laser line used in commercial IRMPD-FTICR instruments?

To assess the reproducibility of these fragment ratios, the experiment was repeated five times for each disaccharide isomer. The averages from these five scans and their standard deviations are shown for selected fragment ions for the examples of maltose and cellobiose (Figure 5). It is clear that all the fragments display a wavelength-dependent behavior that is highly reproducible. These relative standard deviations were comparable for all disaccharides examined.

Irradiation Time and Fluence. Fragment ion abundances in stochastic fragmentation methods are dependent on a host of parameters, including the excitation energy, the time scale of ion excitation, and the pre-excitation internal energy of the ion.[58] In IR-MPD, the most obvious experimental parameters that can be modified are the laser irradiation time[59] and the laser fluence.[48] The free electron laser is a pulsed laser that delivers pulse trains at various repetition rates (see Experimental Section). To probe the effect of ion heating from one macropulse to the next, the ion cloud was irradiated with multiple macropulses (either 10 or 20)

(58) Laskin, J.; Denisov, E.; Futrell, J. H. *Int. J. Mass Spectrom.* **2002**, *219*, 189−201.

(59) Crowe, M. C.; Brodbelt, J. S.; Goolsby, B. J.; Paul, H. *J. Am. Soc. Mass Spectrom.* **2002**, *13*, 630−649.

Table 1. Relative IR-MPD Fragment Intensities at a Wavelength of 9.2 μm[a]

m/z	kojibiose α1−2	sophorose β1−2	nigerose α1−3	laminaribiose β1−3	maltose α1−4	cellobiose β1−4	isomaltose α1−6	gentiobiose β1−6
331	0	0	45	22	18	24	8	11
289	0	0	0	0	34	19	95	64
259	0	0	9	22	0	0	50	42
229	96	100	0	0	3	8	31	52
187	80	11	45	23	95	28	100	25
169	53	58	100	100	100	100	57	100
127	100	40	47	36	62	26	90	5
109	47	16	53	17	33	10	39	10
97	66	28	57	35	34	19	43	19
91	65	20	80	23	35	11	42	10
67	53	23	46	19	17	10	21	10

[a] Numbers represent the relative ion intensities recorded in the *m/z* channels indicated in the left-most column.

Table 2. Relative IR-MPD Fragment Intensities at a Wavelength of 9.6 μm[a]

m/z	kojibiose α1−2	sophorose β1−2	nigerose α1−3	laminaribiose β1−3	maltose α1−4	cellobiose β1−4	isomaltose α1−6	gentiobiose β1−6
331	0	0	36	18	9	19	10	9
289	0	0	0	0	25	15	70	53
259	0	0	6	18	0	0	43	32
229	79	100	0	0	1	6	24	37
187	65	10	34	18	87	28	100	21
169	49	70	87	100	100	100	80	100
127	100	44	39	30	61	22	100	12
109	48	20	41	15	42	13	59	13
97	87	41	61	36	52	22	75	23
91	97	28	100	26	55	20	87	20
67	71	34	56	19	30	12	56	16

[a] Numbers represent the relative ion intensities recorded in the *m/z* channels indicated in the left-most column.

at different repetition rates (5 or 10 Hz), while keeping the "total irradiation energy" (i.e., number of macropulses × energy per macropulse; 340 mJ) constant; additional heating produced by subsequent macropulses assumes that ions are in the laser focus for consecutive macropulses, which is nonetheless unlikely, given the imperfect overlap between the FEL and the ion cloud. At a repetition rate of 5 Hz, the ions have a longer delay (200 ms) between multiple macropulses to cool by infrared radiative emission compared to a repetition rate of 10 Hz (100-ms delay). If the heating of ions were to proceed with gradual energy buildup over more than one macropulse, with incomplete radiative cooling between pulses, then changing this repetition rate should affect the relative dissociation product ratios. However, this was clearly not the case (Figure 6A and B). Hence, ion heating with gradual energy buildup over several macropulses is not a major process. Conversely, by reducing the laser fluence (power per macropulse, Figure 6C) by a factor of 2, while keeping the total irradiation energy constant, the relative IR-MPD product ion abundances do change significantly. In particular, the anomer-specific fragments *m/z* 169 and 187 are increased relative to the cross-ring cleavage products *m/z* 289 and 67. It is clear that a higher laser fluence leads to a buildup of higher internal energies of the ions (above their dissociation thresholds); thus, the higher barrier dissociation pathways become increasingly available. Note that IR-MPD is, however, not a linear process, where doubled laser fluence would be expected to lead to a doubling of the absorbed energy. Also, the ratio of the anomer-specific fragments *m/z* 169 and 187 was hardly affected by the experimental parameters, an observation worthy of note for anomeric discrimination.

Sequential Fragmentation. The effect of sequential dissociation was investigated by continuously ejecting some fragment ions to determine whether the abundances of smaller mass fragment ions were affected. For example, in the case of lithiated maltose, the fragment ions *m/z* 289, 187, and 169 were separately ejected (by continuous ejection) and the effect of the abundance on the lower mass ions (<160 *m/z*) *m/z* 127, 97, and 67 was determined (see Figure 7). While the ejection of *m/z* 289 and 169 had no or very little effect on the abundances of the smaller fragments, the continuous ejection of *m/z* 187 caused a decrease. This suggests that sequential fragmentation takes place in the IR-MPD experiments, especially with respect to *m/z* 187 and the lower mass fragments. As shown before, the relative fragmentation is strongly dependent on the laser fluence; hence, controlling the fluence should allow control over sequential fragmentation and thereby permit reproducibility of the spectral "fingerprints". In contrast, previous CID studies with lithium-adducted disaccharides in a Paul trap established that product ions of disaccharides were derived almost exclusively directly from the precursor ions using double-resonance techniques.[8]

Reducing End Anomers. Disaccharides in solution that have a free reducing end usually exist in more than one form; with glucose as the reducing sugar, the α- and β-pyranose forms are the most abundant. It is unclear as to whether each form can coordinate with lithium at different sites, but it is quite possible

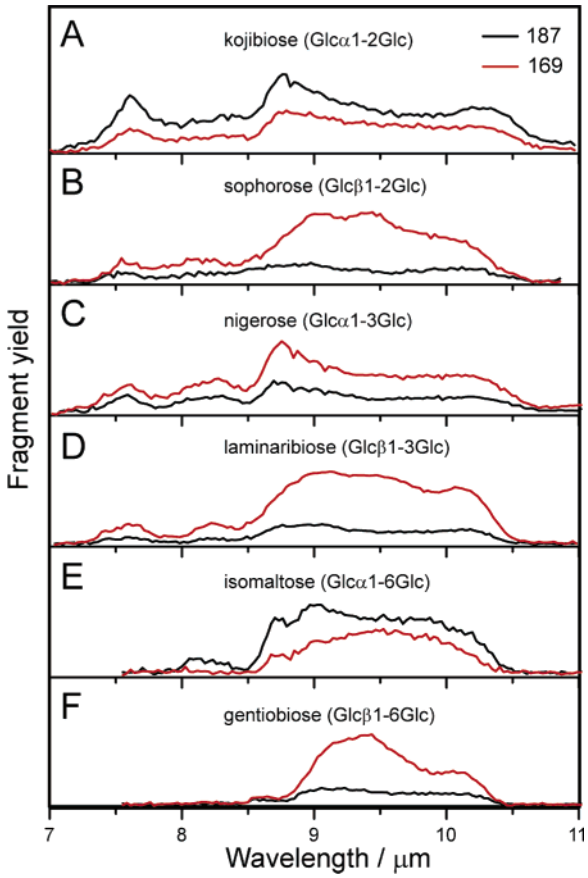

Figure 4. Comparisons of the *m*/*z* 169 and 187 product ion yields over the IR irradiation range from 7 to 11 μm for (A) kojibiose, (B) sophorose, (C) nigerose, (D) laminaribiose, (E) isomaltose, and (F) gentiobiose.

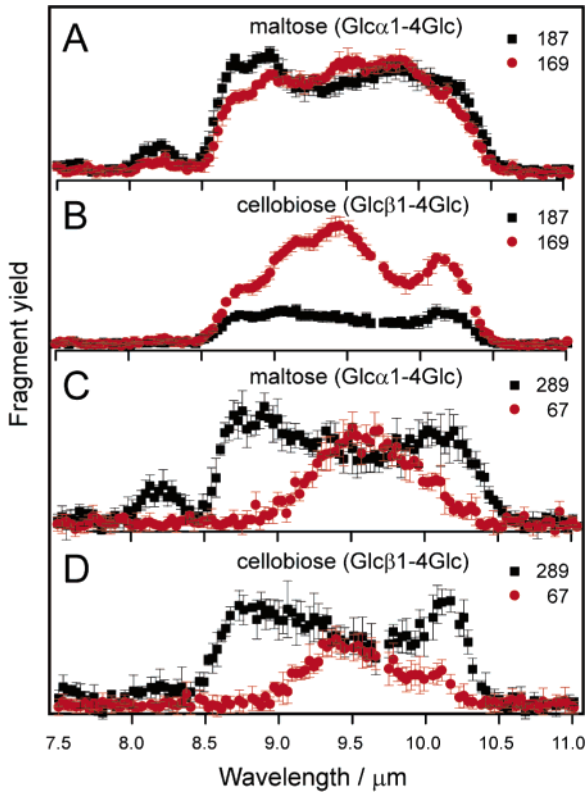

Figure 5. Standard deviation of wavelength-dependent IR-MPD fragment channel intensities for (A) maltose *m*/*z* 187 and 169, (B) cellobiose *m*/*z* 187 and 169, (C) maltose *m*/*z* 289 and 67, and (D) cellobiose *m*/*z* 289 and 67 ions. Note that *m*/*z* 187 and 169 ions were more abundant and hence show less relative deviation as compared to the less abundant *m*/*z* 289 and 67 ions.

that more than one configuration is being simultaneously analyzed. However, whatever the ratios of these precursor ions generated in these experiments, they should remain constant during the electrospray process. The only variable that changes over the course of an accumulated spectrum is the IR wavelength, and the generated IR spectra are clearly highly reproducible.

Total IR-MPD Spectra of Gas-Phase Lithiated Disaccharides. In Figure 8, the IR-MPD spectra of the lithiated disaccharides are presented as the total yield (i.e., the sum of the intensities of all fragment ions divided by the sum of all ions) as a function of wavelength. All lithiated disaccharides show a broad main absorption band between 8.5 and 10.5 μm, and the maximum IR-MPD yield is generally in the 9−9.6-μm range. The 1−2- and 1−3-linked disaccharides also have appreciable bands at ~7.5 and 8.1 μm. These bands are clearly much weaker for the 1−4- and 1−6-linked disaccharides and may have some specificity for the linkage pattern. In conventional FTICR instruments equipped with an IR-MPD option, a commercial nontunable CO_2 laser is used at a fixed wavelength of 10.6 μm. For comparison, the 10.6-μm line is indicated with a dashed line in the IR-MPD spectra. Clearly, this wavelength is at the very edge of the main absorption band and dissociation is poor. At 10.6 μm, the abundances of ions that distinguish α- and β-anomers (*m*/*z* 169 and 187) were low and anomers could not be differentiated.

Comparison to IR Spectra of Condensed-Phase Sugars. Differences have been observed in the infrared absorption spectra of sugars in liquid solvents and in the solid phase (pressed salt pellets or Nujol mulls) going back to detailed investigations in the 1950s. Although many of the absorption bands have proven difficult to assign due to spectral overlap, certain bands were assigned in studies based on comparisons between monosaccharide glycosides that varied solely in their anomeric configuration, in one epimeric position in the sugar ring, or in studies that employed isotopic substitution at specific sites in sugar molecules.[60−63] Most relevant to our current observations were that *anomers* showed differences in the IR spectral region described in the excellent review of Tipson and Parker[61] as the "fingerprint region" from 7 to 11 μm. While a comparable IR absorbance for oligosaccharides is found in the OH stretching band region (i.e., 3 μm), the fingerprint region shows the most marked spectral differences between isomers.[60−63]

These same differences would be anticipated in the gas phase for ionic species, with three provisos: (1) Many bands would be shifted to different fundamental frequencies due to the absence of intermolecular interaction (solvent or solid phase) effects. (2) Li^+ attachment could have significant effects on these frequencies.

(60) Barker, S. A.; Moore, R. H.; Stacey, M.; Whiffen, D. H. *Nature* **1960**, *186*, 307−308.
(61) Tipson, R. S.; Parker, F. S. In *The Carbohydrates, Chemistry and Biochemistry*; Pigman, W., Horon, D., Eds.; Academic Press: New York, 1980; pp 1394−1436.
(62) Back, D. M.; Polavarapu, P. L. *Carbohydr. Res.* **1983**, *121*, 308−311.
(63) Mathlouthi, M.; Koenig, J. L. *Adv. Carbohydr. Chem. Biochem.* **1986**, *44*, 7−89.

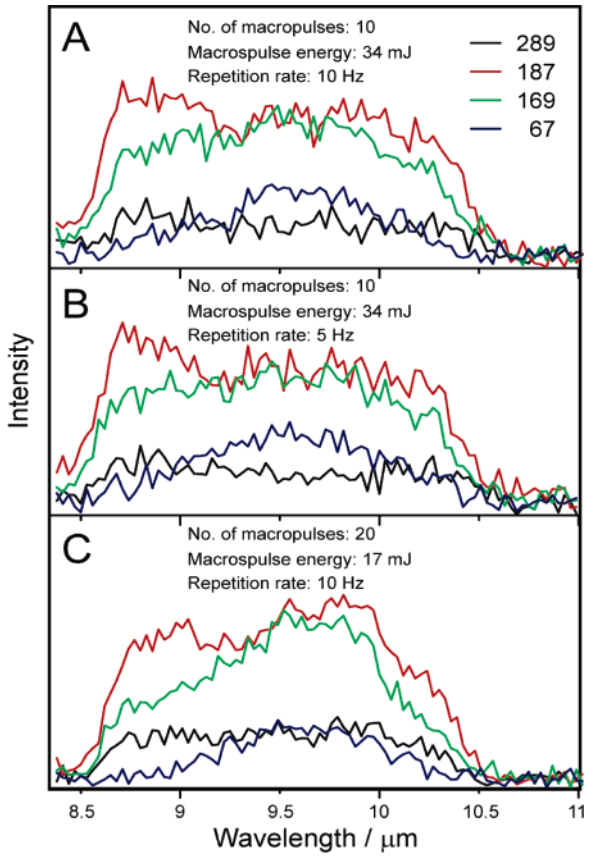

Figure 6. Selected IR-MPD product abundances for lithiated maltose for different laser settings: (A) 10 macropulses of 34 mJ each at a repetition rate of 10 Hz (1 s total time); (B) 10 macropulses of 34 mJ each at a repetition rate of 5 Hz (2 s total time); and (C) 20 macropulses of 17 mJ each at a repetition rate of 10 Hz (1 s total time). Note that the macropulse energy does vary slightly over this wavelength region (i.e., from 32 to 37 mJ) but that the ion intensities are normalized to take this into account.

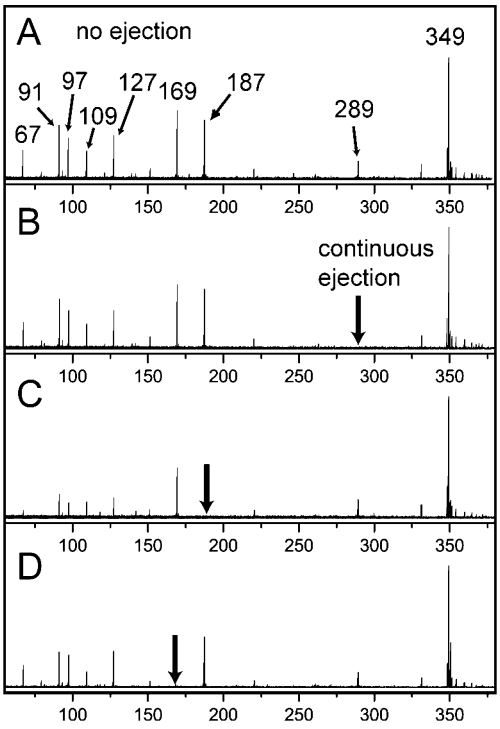

Figure 7. IR-MPD mass spectra of maltose (Glcα1−4Glc) at 9.5 μm (A) without ejection of product ions and with continuous ejection at *m*/*z* (B) 289, (C) 187, and (D) 169.

(3) The absorption frequencies themselves typically shift as multiple IR photons are absorbed, referred to as anharmonic shifting.[30,64] From the practical perspective, any differences in IR absorption spectra between isomers could potentially be exploited in variable-wavelength IR-MPD, an advantage that should be generally applicable to isomers of all types of molecules.

Dynamics of IR-MPD. In the gas phase at high vacuum in an FTICR instrument, collisional relaxation is minimal, wherefore the internal energy of the ions can build up to high levels (i.e., few eV). Equilibration of this intramolecular energy through redistribution over different vibrational modes is very rapid, as evidenced by measured coherence transfer rates in the sub-picosecond to picosecond time frame in two-dimensional IR spectroscopy.[65−67] Conversely, measurements of the rates of metastable decay of lithium-cationized oligosaccharides after excitation to high enough energy levels to cause dissociation in an FTICR instrument,[42] are in the range of a few milliseconds, or many orders of magnitude slower than intramolecular vibrational redistribution. Differences in fragmentation of isomers partly reflect differences in the rates of absorption of photons at different wavelengths, with intramolecular energy building up rapidly compared to rates of dissociation. Once a threshold energy level is reached, dissociation can occur initially via the lowest energy dissociation channels. During the 5 μs of a FELIX macropulse, the number of photons absorbed may excite ions to internal energies that significantly exceed this threshold energy level. If so, then higher energy dissociation channels are available that compete with the lower energy channels. By analogy, the fragmentation dynamics of competing dissociation pathways in protonated peptides have been the subject of a number of theoretical studies involving unimolecular RRKM formalism.[58,68,69] These dynamics depend on a host of experimental parameters, including the total vibrational energy deposited in the ion, the time scale of ion excitation, and the pre-excitation internal energy of the ion,[58] as well as the structure of the ions.[70] No such detailed theoretical studies have yet been carried out on oligosaccharides. However, CID studies on chloride-tagged disaccharides have shown that the ratios of fragments change as a function of the collision energy and that there are differences in the ratios between different anomers.[54] Also worth mentioning are slow heating methods,[71] where the excitation times are defined roughly

(64) Oomens, J.; Tielens, A. G. G. M.; Sartakov, B. G.; von Helden, G.; Meijer, G. *Astrophys. J.* **2003**, *591*, 968−985.
(65) Hamm, P.; Lim, M.; Hochstrasser, R. M. *J. Phys. Chem. B* **1998**, *102*, 6123−6138.
(66) Hochstrasser, R. M.; Ge, N.-H.; Sandrasegarum, G.; Zanni, M. T. *Bull. Chem. Soc. Jpn.* **2002**, *75*, 1103−1110.
(67) Fulmer, E. C.; Mukherjee, P.; Krummel, A. T.; Zanni, M. T. *J. Chem. Phys.* **2004**, *120*, 8067−8078.
(68) Paizs, B.; Suhai, S. *Rapid Commun. Mass Spectrom.* **2002**, *16*, 375−389.
(69) Hu, Y. J.; Hadas, B.; Davidovitz, M.; Balta, B.; Lifshitz, C. *J. Phys. Chem. A* **2003**, *107*, 6507−6514.
(70) Tsaprailis, G.; Nair, H.; Somogyi, A.; Wysocki, V. H.; Zhong, W.; Futrell, J. H.; Summerfield, S. G.; Gaskell, S. J. *J. Am. Chem. Soc.* **1999**, *121*, 5142−5154.
(71) McLuckey, S. A.; Goeringer, D. E. *J. Mass Spectrom.* **1997**, *32*, 461−474.

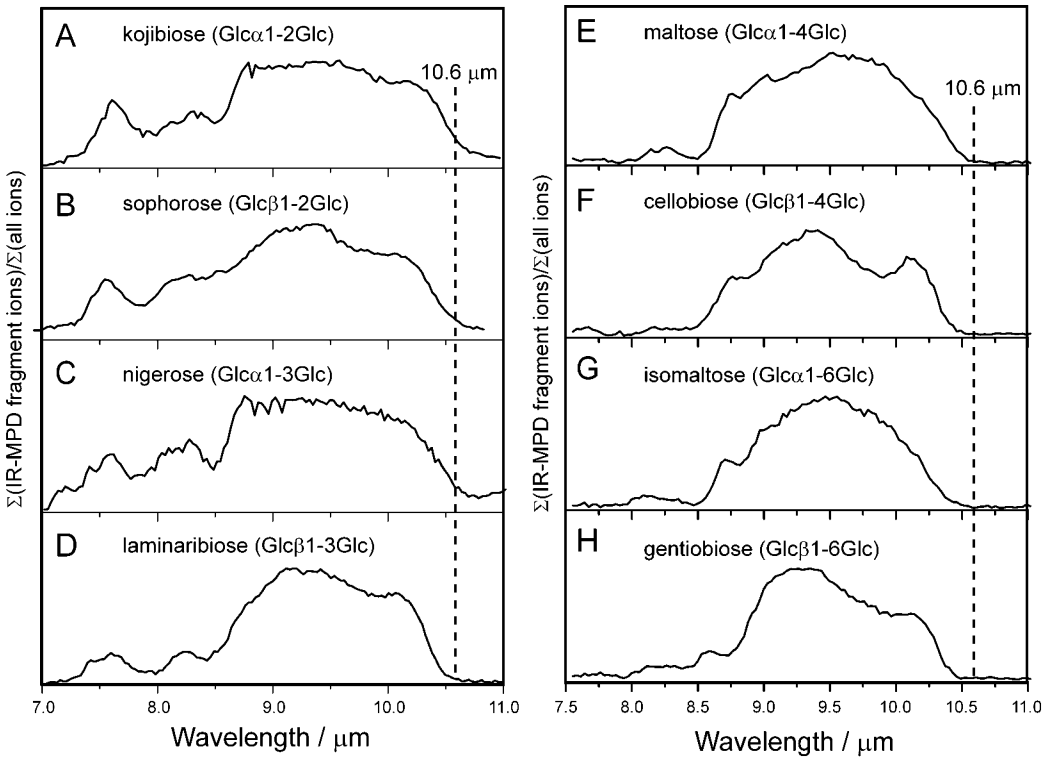

Figure 8. Overall IR-MPD spectra of different lithium-cationized disaccharides representing the sum of all product ions divided by the sum of all ions as a function of IR wavelength. The different disaccharides are shown in each panel.

in the time frame of 10 ms or greater, making excitation and dissociation concurrent events.

CONCLUSIONS

Combining high-resolution FTICR with variable-wavelength IR-MPD in two-dimensional spectra provides several advantages for differentiating between isomeric molecules compared to conventional mass spectrometric fragmentation techniques such as collision-induced dissociation. (1) The variable wavelength adds an extra dimension to the dissociation spectra, which are shown to be unique for each isomer, thus representing a true fingerprint. Disaccharides varying solely in their anomeric configuration were clearly distinguished, where β-anomers consistently had much higher 169/187 ratios than α-anomers in the range of 9.0−9.6 μm. Where isomers showed differences in the presence or absence of specific product ions, as occurred in comparisons between disaccharides having different linkages, discriminating between them was simple, in agreement with studies that previously employed CID.[7,8] (2) Since FTICR experiments are carried out under high vacuum, collisional effects can be kept to a minimum. From the perspective of reproducibility, the power, wavelength, and timing of lasing pulses are the key instrumental controls and transfer of energy to or from a bath gas can be neglected. (3) The ability to tune the free electron laser clearly demonstrated that wavelengths other than the 10.6-μm band used in commercial FTICR instruments need to be exploited to optimize isomeric discrimination by IR-MPD. Thus, a CO_2 laser equipped with moderate tuning capabilities through the use of gratings, other bands, or isotopomers of CO_2, would be far preferable to the single wavelength currently commercially available for FTICR instruments and should be generally propitious for IR-MPD experiments. With respect to larger oligosaccharides, the number of isomeric conformers becomes prohibitive, and hence, one strategy could involve fragmenting precursor ions to disaccharide subunits, which would then be characterized by 2D IRI-MS.

ACKNOWLEDGMENT

This work is part of the research program of FOM, which is financially supported by the "Nederlandse Organisatie voor Wetenschappelijk Onderzoek" (NWO). The skillful assistance of the FELIX staff is greatly acknowledged. Construction and shipping of the FTICR mass spectrometer were made possible with funding from the National High Field FTICR facility (Grant CHE-9909502) at the National High Magnetic Field Laboratory, Tallahassee, FL. Research was supported in part by NSF Grant CHE-0137986 (B.B.). J.J.V. was supported in part by a Dissertation Enhancement Award (OISE-0443540) from the National Science Foundation. We thank Geoffrey Armstrong for computer visualization of 2D spectra and Han de Witte for technical support.

Received for review October 31, 2005. Accepted December 8, 2005.

AC0519458